Archives of Biochemistry and Biophysics 502 (2010) 53–59

Contents lists available at ScienceDirect

Archives of Biochemistry and Biophysics

journal homepage: www.elsevier.com/locate/yabbi

Comparison of solution and crystal properties of Co(II)–substituted human carbonic anhydrase II

Balendu Sankara Avvaru [a], Daniel J. Arenas [b], Chingkuang Tu [c], D.B. Tanner [b], Robert McKenna [a,*], David N. Silverman [a,c,**]

[a] Department of Biochemistry and Molecular Biology, University of Florida, Gainesville, FL 32610, USA
[b] Department of Physics, University of Florida, Gainesville, FL 32610, USA
[c] Department of Pharmacology, University of Florida, Gainesville, FL 32610, USA

ARTICLE INFO

Article history:
Received 26 May 2010
and in revised form 9 July 2010
Available online 14 July 2010

Keywords:
Carbonic anhydrase
Metalloenzyme
Cobalt substitution
Crystallography
Carbon dioxide

ABSTRACT

The visible absorption of crystals of Co(II)–substituted human carbonic anhydrase II (Co(II)–HCA II) were measured over a pH range of 6.0–11.0 giving an estimate of pK_a 8.4 for the ionization of the metal-bound water in the crystal. This is higher by about 1.2 pK_a units than the pK_a near 7.2 for Co(II)–CA II in solution. This effect is attributed to a nonspecific ionic strength effect of 1.4 M citrate in the precipitant solution used in the crystal growth. A pK_a of 8.3 for the aqueous ligand of the cobalt was measured for Co(II)–HCA II in solution containing 0.8 M citrate. Citrate is not an inhibitor of the catalytic activity of Co(II)–HCA II and was not observed in crystal structures. The X-ray structures at 1.5–1.6 Å resolution of Co(II)–HCA II were determined for crystals prepared at pH 6.0, 8.5 and 11.0 and revealed no conformational changes of amino-acid side chains as a result of the use of citrate. However, the studies of Co(II)–HCA II did reveal a change in metal coordination from tetrahedral at pH 11 to a coordination consistent with a mixed population of both tetrahedral and penta-coordinate at pH 8.5 to an octahedral geometry characteristic of the oxidized enzyme Co(III)–HCA II at pH 6.0.

Introduction

Intense discussion has been given to the similarity and differences between crystal and solution structures in understanding enzyme properties and catalytic mechanisms [1,2]. We report here a specific example in which different sample conditions results in different properties for solution and crystal states of carbonic anhydrase II (HCA II)[1]. HCA II relies on a zinc-bound hydroxide to catalyze the hydration of carbon dioxide forming bicarbonate and a proton. The active-site zinc can be removed with chelators and replaced with a variety of metal ions (Co, Mn, Ni, Cu, Fe, Cd) [3,4]. However, the cobalt–substituted enzyme (Co(II)–HCA II) is the only derivative with catalytic activity comparable to the native zinc-containing enzyme [5].

The zinc in the native enzyme is tetrahedrally coordinated by three first-shell amino acid ligands (His94, His96 and His119) and a single solvent molecule (Fig. 1). The crystal structure of Co(II)–HCA II shows minimal changes in amino-acid backbone conformation as a result of the metal substitution [6,7]. The cobalt ion, like the zinc, is coordinated by the same three first-shell histidine ligands although the number and orientation of the solvent ligands are pH dependent. Hakansson et al. previously solved crystal structures of Co(II)–HCA II at pH values of 6.0 and 7.8 [7]. They found sulfate, an inhibitor of CA, from the crystallization precipitant solution was bound to Co(II) in the structure at pH 6.0 displacing the metal bound solvent with geometry about the cobalt approximately penta-coordinate, whilst Co(II) at pH 7.8 was reported to be in tetrahedral coordination.

An advantage of the study of Co(II)–HCA II is that its visible absorption spectrum is very sensitive to pH. Specifically, the spectra fit a two-state model in which the low pH and high pH forms are related to changes in coordination about the cobalt and changes in the protonation state of the aqueous ligand of the cobalt [3,4]. The data indicate an equilibrium between high and low pH forms, and the spectral changes parallel changes in catalytic activity [5]. More detailed solution studies show the titration curve is complex consistent with a smaller influence of other ionizable groups near the active site [4,8]. The visible spectrum of Co(II)–CA observed at high pH shows much stronger absorbance at 640 nm ($\varepsilon \sim 300\ M^{-1}\ cm^{-1}$) than that at low pH ($\varepsilon \sim 50\ M^{-1}\ cm^{-1}$). The optical spectra of inhibited complexes of CA suggest that the high pH form is associated with a near tetrahedral coordination

* Corresponding author. Address: Department of Biochemistry and Molecular Biology, College of Medicine, University of Florida, Box 100245, Gainesville, FL 32610, USA. Fax: +1 352 392 3422.
** Corresponding author at: Department of Pharmacology, College of Medicine, University of Florida, Box 100267, Gainesville, FL 32610, USA. Fax: +1 352 392 9696.
E-mail addresses: rmckenna@ufl.edu (R. McKenna), silvrmn@ufl.edu (D.N. Silverman).

[1] *Abbreviation used:* HCA II, human carbonic anhydrase II.

0003-9861/$ - see front matter © 2010 Elsevier Inc. All rights reserved.
doi:10.1016/j.abb.2010.07.010

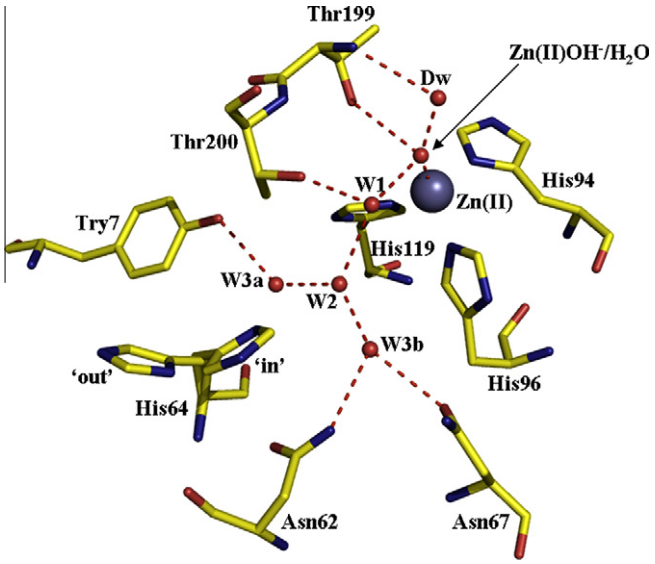

Fig. 1. The active site of Zn(II)–HCA II. The amino acids lining the hydrophilic side of the active site are represented as sticks (yellow: carbon; red: oxygen; blue: nitrogen). The waters are represented as red spheres and the network of possible hydrogen bonds are depicted as red dashes. The Zn(II) is represented as a gray sphere. Figure made using PyMOL (DeLano Scientific). (For interpretation of the references in colour in this figure legend, the reader is referred to the web version of this article.)

about the cobalt, and the low pH form is a five-coordinate structure [9].

The aim of this study is to take advantage of the visible spectra of Co(II)–HCA II to compare in solution and in crystals the ionization state of the active site, that is the pK_a of the cobalt-bound water. The visible absorption spectra of crystals of Co(II)–HCA II as well as the crystal structures at pH values of 6.0, 8.5 and 11.0 are reported. These are compared with solution properties of Co(II)–HCA II including catalytic activity and pK_a of the catalysis. Whereas many studies in the literature are consistent with a p*K*a near 7 for the protolysis of the metal-bound water in HCA II [4,5,10,11], the crystals of Co(II)–HCA II show a spectroscopic pK_a of 8.4. This difference is attributed to an ionic strength effect caused by the presence of a high concentration of citrate ions in forming crystals. Understanding this difference in pK_a between crystal and solution forms of carbonic anhydrase has implications in interpreting pH dependent changes in crystal structures of carbonic anhydrase, such as the pH dependent orientation of the proton shuttle residue His64 [12,13], and the observation from neutron diffraction of a metal-bound water molecule in HCA II [14].

Materials and methods

Expression and preparation of HCA II

The plasmid encoding HCA II was transformed into *Escherichia coli* BL21 cells through standard procedures and the transformed cells were expressed at 37 °C in LB medium containing 100 μg/ml ampicillin. HCA II production was induced by the addition of isopropyl thiogalactoside to a final concentration of 1 mM at an OD_{600} of 0.6. The cells were harvested 4 h after induction. The cell pellets were lysed and holo-HCA II was purified through affinity chromatography [15].

The zinc was removed from holo-HCA II by chelation at 20 °C using 100 mM pyridine-2,6-dicarboxylic acid and 25 mM MOPS at pH 7.0. After 8 h the enzyme was buffer exchanged against 50 mM Tris at pH 7.8 to remove the metal and chelating agent. The loss of enzyme activity of the apo-enzyme was verified through ^{18}O exchange [16]. The enzyme activity was revived through the addition of 1 mM $ZnCl_2$, attributing the loss of activity to the absence of zinc rather than to the denaturation of the enzyme.

Preparation of Co(II)–HCA II crystals

Crystals of apo-HCA II were obtained through the hanging drop vapor diffusion method. Ten microliters drops of 5 μl of protein and 5 μl precipitant were equilibrated against 1 ml precipitant solution (1.4 M sodium citrate; 100 mM Tris–HCl; pH 9.0) at room temperature (~20 °C). The apo-HCA II crystals were transferred into soaking solutions of cobalt salt (100 mM $CoCl_2$; 1.4 M sodium citrate; 50 mM Tris–Cl; 50 mM 3-(cyclohexylamino)propanesulfonic acid (CAPS)) with pH values of 6.0, 8.5 and 11.0, respectively. The crystals were incubated for 2–3 days to let the Co(II) ion infuse into the active site. Each crystal was then individually sealed in a quartz capillary tube (outer diameter: 1.0 mm; wall thickness: 0.01 mm) with a small quantity of soaking solution at one end to maintain the vapor pressure and prevent crystal dehydration.

Optical measurements

The UV/VIS transmittance of crystals in the capillaries was measured using a Zeiss MPM 800 microscope photometer at room temperature (RT) using a beam spot of dimensions less than $100 \times 100\ \mu m^2$. Due to the refractive index of the round capillary tubes and of the crystals, refraction can change the beam path, resulting in a portion of the beam missing the detector. To minimize this refraction, the tubes were placed such that the surface of the capillary tube was normal to the beam path.

For the analysis, it was important to show that any amount of light lost due to refraction was independent of frequency. First, the transmittance of empty capillary tubes was measured and found to be constant in frequency (non-dispersive). Then the transmittance of crystals contained in capillaries was corrected using the transmittance of the empty capillary tube. These results showed that the transmittance at longer wavelengths ($\lambda > 800$ nm) was close to 1 which suggested that the amount of light lost to refraction was minimal (<3%). As a further check, the transmittance of the crystals was measured for different orientations of the crystal and capillary tube, and it was confirmed that the frequencies of the transmission dips (associated with absorption peaks) were independent of the orientation of the capillary in the beam. Therefore it was concluded that the placement of crystals in capillary tubes did not introduce a frequency-dependent error and did not affect the positions and relative intensities of the absorbance peaks.

The absorbance (A) is dependent on the thickness (d) of the crystals and the extinction coefficient (α) characteristic of the material and is defined as $A = \alpha d$. The absolute extinction coefficients of different crystals could not be compared due to the variation in thickness and shapes of the crystals used. Therefore, the reported extinction coefficients are given in arbitrary units. At lower wavelengths, the visible spectra observed were dominated by nonspecific loss of transmission due to light scattering. To subtract this background, the absorption data for each crystal were first fitted to a Lorentzian oscillator model for interband transitions [17]. Then, the high frequency oscillators ($\lambda < 400$ nm; $\upsilon > 25000\ cm^{-1}$) were subtracted from the original data.

X-ray data collection

X-ray diffraction data sets of Co(II)–HCA II crystals at pH values 6.0, 8.5 and 11.0 were collected in-house at RT using an *R*-AXIS IV^{++}

image plate system with Osmic mirrors and a Rigaku RU-H3R Cu rotating anode (λ = 1.5418 Å) operating at 50 kV and 100 mA. The image plate-crystal distance was set at 80 mm. The oscillation steps were 1° with a 7 min exposure per image. X-ray data processing and scaling was performed using HKL2000 [18].

All three data sets were solved and refined using SHELX97 [19]. The data were phased using the wild type HCA II coordinates (PDB Accession Code: 2CBA) [6], with all the solvent, and the Zn(II) active site metal ion removed to avoid model bias. Five percent of unique reflections were randomly selected to serve the purpose of R_{free} calculations. The model refinement using SHELXL97 proceeded initially with the data set from 20.0 to 2.0 Å resolution. The protein model was visualized and refined using the molecular graphics program COOT [20]. Subsequent cycles of refinement included the incorporation of cobalt, solvent and dual conformers of side chains. The protein geometry was defined by the default constraints of conjugate-least squares (CGLS) mode in SHELXL97. Each round of CGLS comprised of 15 cycles of refinement. $2F_o–F_c$ and $F_o–F_c$ maps were manually inspected after each successive round of CGLS for further fine-tuning of the model and the incorporation of solvent molecules. Thereafter, the refinement of the structures of Co(II)–HCA II was scaled up to respective maximum resolutions. Table 1 provides the final data collection and refinement statistics for the structures determined at pH 6.0, 8.5 and 11. The atomic coordinates for Co(II)–HCA II at pH 6.0, 8.5 and pH 11.0 have been deposited with the Protein Data Bank as entries 3KOI, 3KOK, and 3KON, respectively.

Catalysis

The rate of catalyzed hydration of CO_2 was measured by the ^{18}O exchange method that has been used extensively to study this reaction [16,21]. The method uses membrane inlet mass spectrometry to determine the rate of depletion of ^{18}O from CO_2 as this isotope is exchanged into water where it is essentially infinitely diluted by $H_2{}^{16}O$. In this study, the method was used to measure activity in the presence of large concentrations of sodium citrate.

Results

Visible absorption

Absorption spectra of crystals of Co(II)–HCA II are shown in Fig. 2. The peak at 640 nm is a major pH-dependent absorbance for Co(II)–substituted CA II. Although there is considerable scatter in these spectra, the absorbance at 565 nm appears to correspond to the isosbestic point that is observed at this wavelength in solution phase, having an identical absorbance for a high pH and a low pH form of Co(II)–substituted CA II [3–5]. Due to the differing sizes and volumes of the crystals, a direct comparison between the extinction coefficients was not possible. However, the data could be normalized to the isobestic point at 565 nm (Fig. 2). Fig. 3 shows that the ratio of extinction coefficients $\varepsilon_{640}/\varepsilon_{565}$ could be fitted to a single ionization, for crystalline Co(II)–HCA II prepared from precipitant solutions containing 1.4 M citrate, for Co(II)–HCA II in solution containing 0.8 M sodium citrate, and for Co(II)–HCA II in solution containing 20 mM potassium sulfate, but no citrate, as measured by Taylor et al. [22].

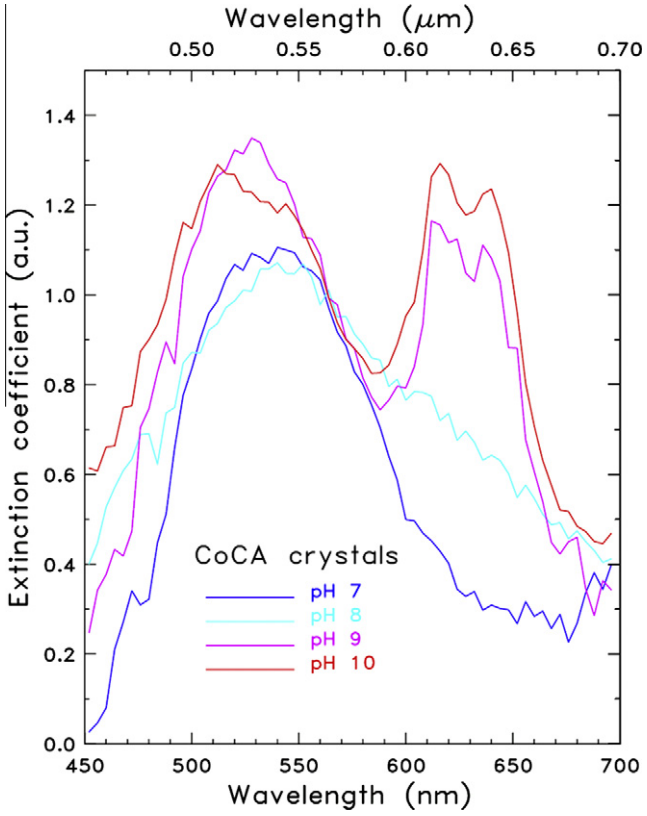

Fig. 2. The pH profiles for the extinction coefficients (a.u. is arbitrary units) of crystals of Co(II)–HCA II (dimensions approximately 0.2 × 0.2 × 0.2 mm^3) mounted in quartz capillary tubes (outer diameter 1.0 mm, wall thickness 0.01 mm). The UV/VIS transmittance was measured using a Zeiss MPM 800 microscope photometer at room temperature using a beam spot of dimensions less than 100 × 100 μm^2. The extinction coefficient of each crystal was scaled to be unity at the isosbestic point at 565 nm.

Table 1
Data-collection and refinement statistics of crystal structures of Co(II)–HCA II at pH 6.0, 8.5 and 11.

	pH 6.0	pH 8.5	pH 11.0
Unit cell dimensions, *a*, *b*, *c* (Å), β (°)	42.8,41.7,72.9,104.6	42.6,41.8,72.8,104.6	42.7,41.7,72.8,104.6
Resolution (Å)	50–1.6 (1.65–1.60)	50–1.5 (1.55–1.50)	50–1.5 (1.55–1.50)
# of unique reflections	29472 (3021)	36608 (3472)	38235 (3815)
Completeness (%)	92.4(90.5)	95.8 (91.8)	97.9 (98.1)
Redundancy	2.4 (2.0)	3.5 (2.8)	3.3 (3.1)
R_{symm}[a]	8.0 (43.0)	7.4 (44.0)	6.5 (32.0)
$I/\sigma(I)$	16.0 (5.0)	28.0 (4.0)	20.0 (6.0)
R_{cryst}[b]/R_{free}[c]	18.9/21.5	19.4/22.7	20.1/23.5
Ramachandran statistics (%) Favored, additionally, and generously allowed regions	88, 11.5, 0.5	88, 11.5, 0.5	88, 11.5, 0.5
# of protein/solvent atoms	2048/138	2068/223	2068/212
Average B factors(Å^2) main/side chain	11.7/17.4	15.9/21.0	14.2/18.8
Co/solvent	5.0/21.0	8.8/30.2	6.6/26.0

Values in parentheses refer to the highest resolution bin. [a]$R_{symm} = \Sigma|I - \langle I\rangle|/\Sigma\langle I\rangle \times 100$. [b]$R_{cryst} = \Sigma\ |F_o|-|F_c|/\Sigma|F_{obs}| \times 100$. [c]$R_{free}$ is calculated in same manner as R_{cryst}, except that it uses 5% of the reflection data omitted from refinement.

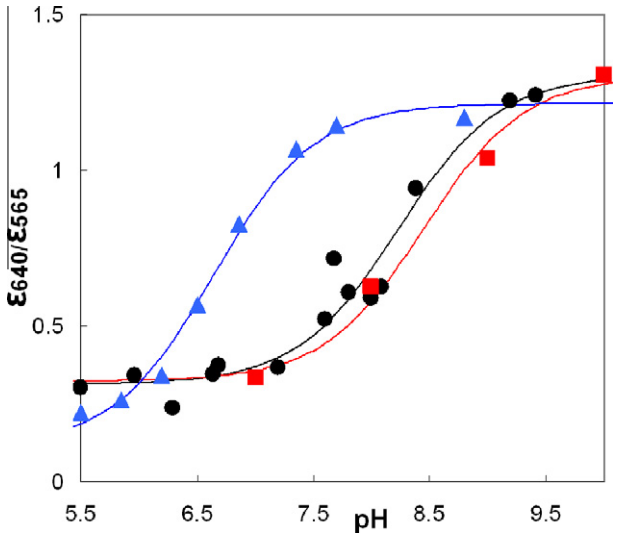

Fig. 3. The pH dependence of the ratio of extinction coefficients $\varepsilon_{640}/\varepsilon_{565}$ for Co(II)–HCA II using (*red*) the data of Fig. 2 for crystalline enzyme; (*black*) solutions of Co(II)–HCA II containing 0.8 M sodium citrate, 25 mM Tris and 25 mM 2-(*N*-cyclohexylamino)ethanesulfonic acid (Ches); and (*blue*) the data of Taylor et al. [22] for Co(II)–HCA II in solution containing 20 mM potassium sulfate. The absorbance at 640 nm is a major, pH-dependent band, and the absorbance at approximately 565 nm is an isosbestic point for two forms of Co(II)–substituted CA II, one with a water molecule coordinated to the metal and one with hydroxide. The solid lines are fits to a single ionization with values of pK_a of 8.4 ± 0.1 for the crystalline enzyme; 8.3 ± 0.1 for solubilized enzyme in 0.8 M citrate; and 7.2 ± 0.1 for the solubilized enzyme in the absence of citrate.

Fig. 3 shows that the spectroscopic pK_a of the crystalline enzyme prepared in 1.4 M citrate (pK_a 8.4 ± 0.1) and the solubilized enzyme in 0.8 M citrate (pK_a 8.3 ± 0.1) are shifted to a higher value by about 1.2 pK_a units compared with this enzyme in solution in the absence of citrate (pK_a 7.2 ± 0.1). Many labs have measured this pK_a to be near 7.0 for Co(II)–CA II in the absence of citrate and at lower ionic strength [3,22,23]. This shift to a more basic pK_a in the presence of citrate is not due to a specific binding site for citrate at the metal in the active site of the enzyme, as there is no evidence of this from the crystal structures, and citrate does not inhibit this enzyme (see below).

Crystal structures of Co(II)–HCA II

The crystal structures of Co(II)–HCA II at near 1.5 Å resolution were solved and refined using standard procedures; the final refinement statistics are given in Table 1. No significant changes were observed in the protein backbone and side chains due to the substitution of Zn(II) with Co(II) for crystals soaked at pH 6.0, 8.5 and 11.0. The polypeptide backbone of Zn(II)–HCA II (PDB id: 2ili [13]) and the solved Co(II)–HCA II structures were identical, within the resolution limits of the structures, with a *Cα* RMSD less than 0.2 Å. The main observation for this study is that there was no evidence of citrate bound in the active site or on the surface of Co(II)–HCA II. The proton shuttle residue His64 in Co(II)–HCA II was observed in both inward and outward conformations [12] with near equal population of each for all three pH values.

Unlike Zn(II)–HCA II for which there appears to be a single solvent ligand over a range of pH [13,24], significant changes in the coordination number as a function of pH were observed in the first shell of the metal ion in Co(II)–HCA II crystals. The coordination around the cobalt for crystals soaked at pH 11.0 was tetrahedral with three histidine ligands and one solvent molecule (Figs. 4A and 5A; Table 2A). This coordination was identical to that of the tetrahedral coordination of zinc in the native enzyme. The Co(II)–HCA II at pH 11.0 was also similar to the Zn(II)–HCA II in the locations of the second-shell ligands (Dw and W1) and the extended hydrogen bonded water network (W2, W3a and W3b) beyond the second shell (Figs. 1 and 4A).

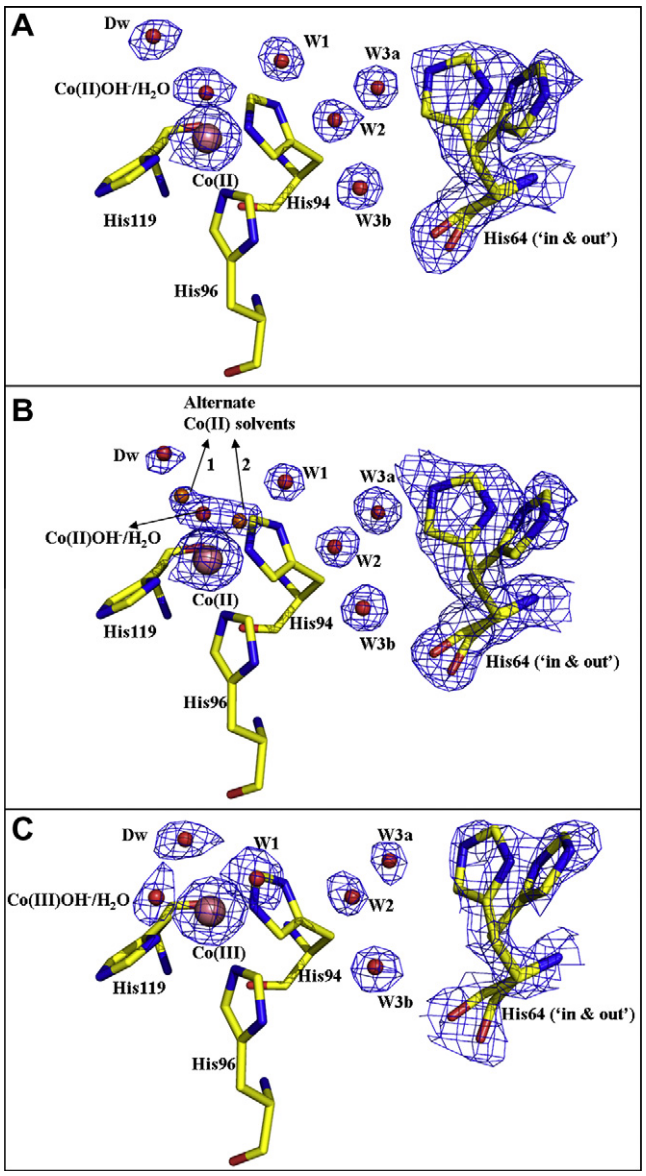

Fig. 4. The active sites of Co(II)–HCA II soaked at (A) pH 11.0; (B) pH 8.5; and (C) pH 6.0. His 64, the proton shuttle residue, was observed in dual inward and outward conformations in the crystal structures. The ordered water structure in the active-site cavity (W1, W2, W3a and W3b) was the same as that observed for the Zn(II)-containing enzyme. All electron density shown is represented by blue as a 1.5σ-weighted $2F_o$–F_c Fourier map. The angles and distances of the first shell cobalt ligation are given in Table 2 and Fig. 5. Figure made using PyMOL (DeLano Scientific).

When the pH of the crystal soaking solution was decreased to 8.5, the coordination around the Co(II) ion appeared to shift from a tetra-coordinated to a coordination resembling more a penta-coordinated species (Figs. 4B and 5B). The electron density maps revealed first-shell solvent ligands that exhibited a volume too large to account for a single solvent molecule but not large enough for two discrete solvent molecules. The structure therefore was refined assuming 50% occupancy for the tetra- and penta-coordinated Co(II) species (Figs. 4B and 5B; Table 2B). The tetra-coordinated species is identical to the tetrahedral geometry of the native Zn(II)-containing enzyme, while the penta-coordinated species is a square pyramidal geometry (Fig. 5B).

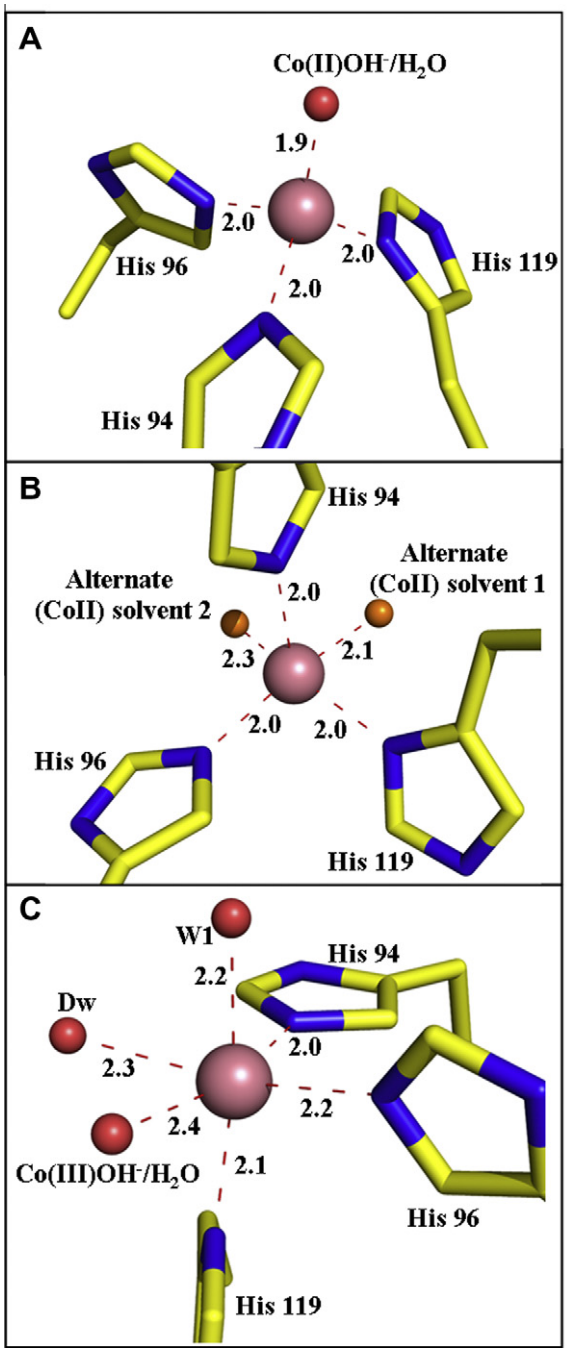

Fig. 5. Cobalt ligand geometry of Co(II)–HCA II soaked at (A) tetrahedral, pH 11.0; (B) pentagonal pH 8.5; and (C) octahedral pH 6.0. Distances (Å) are as depicted. Angles are given in Table 2. Figure made using PyMOL (DeLano Scientific).

Upon further decreasing the pH to 6.0, the cobalt ion assumed a hexa-coordinated ligation (Figs. 4C and 5C; Table 2C). The deep water Dw and W1 from the second ligand shell moved into the first ligand shell. These three first-ligand solvent molecules along with the histidine residues are best described as octahedral geometry (Fig. 5C).

Catalysis

The ^{18}O exchange method was used to measure the rate of hydration of CO_2 catalyzed by human Co(II)–HCA II. This method is based on the depletion of ^{18}O from CO_2 caused by repeated hydration–dehydration cycles as measured by membrane inlet mass spectrometry [21]. This rate of catalyzed hydration was not changed within experimental error when citrate up to 1.3 M was added incrementally to solutions containing Co(II)–HCA II (data not shown). Solutions were maintained at pH 7.6 using 0.1 M Hepes buffer at room temperature. The total concentration of all species of CO_2 was 25 mM.

Discussion

With the accumulation of considerable kinetic and crystallographic information on the carbonic anhydrases, it becomes useful to compare active-site properties in solution and in crystalline states. For example, catalysis by HCA II is very pH dependent [25]; it is necessary to compare crystal structures and kinetic data under similar conditions. We have approached this by placing cobalt at the active site of HCA II and using its visible spectrum as a reporter both in solution and in crystals. Here we point out a significant difference in the pK_a of the cobalt-bound water in crystal versus solution phase. The result we emphasize is that the spectroscopic pK_a of 8.4 for Co(II)–HCA II in the crystal is considerably larger than the often measured pK_a near 7.0 in solution (Fig. 3).

We suggest this difference in pK_a values is due to the significant differences in ionic strength. In this study, citrate was used in the crystallization precipitant solutions because it does not bind in the active site of Co(II)–HCA II, unlike sulfate. We know this because no ordered anion is observed in the crystal structures (Fig. 4), and citrate was shown not to inhibit catalytic activity. In contrast, sulfate was avoided in precipitant solutions, as previous studies of HCA II [26] and Co(II)–HCA II [7] using sulfate resulted in sulfate bound in the active site, which impairs analysis of structure–function data and the role of ordered water in the active-site cavity. We also attempted to find other anions that might be useful in crystallization, however many including malate, oxalate, and glutamate were excluded because they were also all found to be inhibitors of carbonic anhydrase. It is unusual to find an anion that at high concentrations is not an inhibitor of HCA II. The lack of inhibition by citrate is likely due to its intensely negative charge as a trianion; the active site of HCA II near the zinc is narrow and lacking in sufficient positive charge to stabilize a complex with citrate.

The precipitant solution in the current studies contained 1.4 M citrate; this is an ionic strength of 4.8 M. Of course, this does not necessarily reflect the citrate content of the crystals. The visible spectrum of the solution form of Co(II)–HCA II in 0.8 M sodium citrate was fit to a pK_a of 8.3 (Fig. 3), nearly identical to the pK_a obtained from the crystal. By this measure the crystal behaves as if it has the equivalent of 0.8 M citrate. The solution data (Fig. 3) show a pK_a of 7.2 at an ionic strength of 0.06 M due to potassium sulfate.

Despite decades of study on the carbonic anhydrases, there is very little examination of the influence of ionic strength on the properties of the active site such as the pK_a of the aqueous ligand of the metal. This is mainly because of the difficulty in finding anions that do not bind or interact in a manner that perturbs structural or catalytic properties. Jacob et al. [27] measuring the solvent relaxation of protons of an extensively dialyzed sample of Co(II)–bovine CA II, found a pK_a as low as 5.2 at very low ionic strength. This pK_a was observed to be 6.4 in Na_2SO_4 at an ionic strength of 0.3 M. The effect of sulfate is in part a contribution to the ionic strength of solution and in part specific binding of sulfate at the active site as measured by inhibition of catalysis [28]. However, the data indicate and Jacob et al. conclude that the pK_a of the metal-bound water is highly dependent on ionic strength. This conclusion was also reached by Pocker and Miao [29] who determined that the pK_a of the zinc-bound water in bovine CA II in-

Table 2
Geometries of first shell ligands of cobalt in the Co(II)–HCA II crystals at (A) pH 11.0; (B) 8.5; and (C) 6.0.

(A) pH 11.0	Angle *X*–Co–*Y* (°)				
	His94 Nε2	His96 Nε2	His119 Nδ1		
$CoOH/H_2O$	112	116	117		
His94 Nε2		104	112		
His96 Nε2			95		
(B) pH 8.5	His94 Nε2	His96 Nε2	His119 Nδ1	Alternate ligand 1	Alternate ligand 2
$CoOH/H_2O$ (50% occupancy)	111	118	118		
His94 Nε2		104	111	93	90
His96 Nε2			93	160	99
His119 Nδ1				89	152
Alternate ligand 1					71
(C) pH 6.0	His94 Nε2	His96 Nε2	His119 Nδ1	W1	Dw
$CoOH/H_2O$	94	159	95	82	72
His94 Nε2		98	110	85	165
His96 Nε2			97	82	94
His119 Nδ1				165	77
W1					87

creased from 5.9 to 7.0 as the ionic strength of solution was raised from zero to 0.1 M using sulfate.

We examined the crystal structures of Co(II)–HCA II obtained from solutions containing 1.4 M citrate to determine if there are structural changes compared with the many structures reported for HCA II under a variety of conditions. These structures of Co(II)–HCA II are similar in many aspects with structures determined previously [7,30]. The structure at pH 11.0, above the pK_a of the metal-bound water, showed tetrahedral coordination essentially identical with the Zn(II)-containing native enzyme [13,24,31], and is associated with the strong absorbance at 640 nm (Figs. 2 and 5A). The crystal structure at pH 8.5 was refined as an intermediate between tetra- and penta-coordinated species and its absorbance at 640 nm occupies a position between the strong and weak absorbance of tetra- and penta-coordinated species respectively (Fig. 2 and 5B). It is interesting to note that the Co(II)–HCA II crystals at pH 8.5 (Fig. 4B) are near the pK_a at the active site of the crystalline enzyme and lie at an intermediate position between tetra- and penta-coordinated species of Co(II) from the standpoint of structure and visible spectra. Catalysis by Co(II)–substituted CA II is consistent with a two-state model in which only the high pH, tetrahedrally coordinated form is active in the catalytic hydration of CO_2 [5].

The crystal structure at pH 6.0 displays hexa-coordination about the cobalt with metal-solvent ligand distances of less than 2.5 Å (Table 2C and Fig. 5C). The metal ligand distances have relaxed by ~0.3 Å, suggesting a Co(III) state. There is no evidence from previous studies of visible spectra or of crystal structures for a hexa-coordinated species of Co(II)–substituted carbonic anhydrase [4,6,24,31]. On the contrary, the electronic spectra of the oxidized form Co(III)–HCA II have been associated with octahedral complexes [32,33]. In this respect the hexa-coordinate structure at pH 6.0 suggests that the cobalt has been oxidized in our experiments; this is not unexpected since the oxidation of Co(II) is more rapid at low pH. Although the distances of the three solvent ligands ($CoOH^-/H_2O$, W1 and Dw) observed at pH 6.0 were within the first ligand shell, only the $CoOH^-/H_2O$ and W1 were strongly bonded to the metal with B-factors of 4.2 and 6.5 Å^2 respectively. The deep water Dw appears weakly associated to the metal exhibiting a B-factor of 22.5 Å^2.

These results have implications in the interpretation of structures of crystals prepared in solutions containing citrate. For example, in the first structure of a carbonic anhydrase by neutron diffraction, Fisher et al. [14] have prepared crystals of HCA II in precipitant solutions containing an initial concentration of 1.15 M sodium citrate at pH 9.0. The ionization state of the zinc-bound solvent from the neutron diffraction study is more readily understood by assuming that the presence of citrate has increased the pK_a by 1.2 U, as observed in Fig. 3, and by 0.5 to 0.7 U for the increase in dissociation constant of normal acids when deuterated [34]. This brings the estimated pK_a at the metal in HCA II from 7 to near 9 and more readily explains the observed metal-bound D_2O in crystals equilibrated at pH 9.0. The conclusions of this current study need also be considered in assessing the role of the proton shuttle His64 of HCA II which according to crystal structures has a pH dependent conformational change [12,13,35].

Acknowledgments

DJA and DBT acknowledge support by the DOE under contract DE-FG02-02ER45984. This work was supported by NIH Grant GM25154.

References

[1] C.M. Wilmot, A.R. Pearson, Current Opinion in Chemical Biology 6 (2002) 202–207.
[2] R.W. Noble, L.D. Kwiatkowski, H.L. Hui, S. Bruno, S. Bettati, A. Mozzarelli, Protein Science 11 (2002) 1845–1849.
[3] S. Lindskog, Journal of Biological Chemistry 238 (1963) 945–951.
[4] I. Bertini, C. Luchinat, A. Scozzafava, Structure and Bonding 48 (1982) 45–92.
[5] S. Lindskog, Biochemistry 5 (1966) 2641–2647.
[6] K. Hakansson, M. Carlsson, L.A. Svensson, A. Liljas, Journal of Molecular Biology 227 (1992) 1192–1204.
[7] K. Hakansson, A. Wehnert, A. Liljas, Acta Crystallographica Section D-Biological Crystallography 50 (1994) 93–100.
[8] I. Bertini, A. Dei, C. Luchinat, R. Monnanni, Inorganic Chemistry 24 (1985) 301–303.
[9] I. Bertini, G. Canti, C. Luchinat, A. Scozzafava, Journal of the American Chemical Society 100 (1978) 4873–4877.
[10] D.N. Silverman, S. Lindskog, Accounts of Chemical Research 21 (1988) 30–36.
[11] D.N. Silverman, R. McKenna, Accounts of Chemical Research 40 (2007) 669–675.
[12] S.K. Nair, D.W. Christianson, Journal of the American Chemical Society 113 (1991) 9455–9458.
[13] S.Z. Fisher, C.M. Maupin, M. Budayova-Spano, L. Govindasamy, C. Tu, M. Agbandje-McKenna, D.N. Silverman, G.A. Voth, R. McKenna, Biochemistry 46 (2007) 2930–2937.
[14] S.Z. Fisher, A.Y. Kovalevsky, J.F. Domsic, M. Mustyakimov, R. McKenna, D.N. Silverman, P.A. Langan, Biochemistry 49 (2010) 415–421.
[15] R.G. Khalifah, D.J. Strader, S.H. Bryant, S.M. Gibson, Biochemistry 16 (1977) 2241–2247.
[16] D.N. Silverman, Methods in Enzymology 87 (1982) 732–752.
[17] F. Wooten, In Optical Properties of Solids, Academic Press, New York, 260, 1972.

[18] Z. Otwinowski, In An Oscillation Data Processing Suite for Macromolecular Crystallography, Yale University, New Haven, CT, 1992.
[19] G.M. Sheldrick, Acta Crystallographica Section A 64 (2008) 112–122.
[20] P. Emsley, K. Cowtan, Acta Crystallographica Section D-Biological Crystallography 60 (2004) 2126–2132.
[21] D.N. Silverman, C.K. Tu, S. Lindskog, G.C. Wynns, Journal of the American Chemical Society 101 (1979) 6734–6740.
[22] P.W. Taylor, R.W. King, A.S.V. Burgen, Biochemistry 9 (1970) 3894–3899.
[23] I. Bertini, C. Luchinat, A. Scozzafava, Inorganica Chimica Acta-Bioinorganic Chemistry 46 (1980) 85–89.
[24] A. Liljas, S. Lovgren, P.C. Bergsten, U. Carlbom, M. Petef, I. Waara, B. Strandbe, K. Fridborg, L. Jarup, K.K. Kannan, Nature-New Biology 235 (1972) 131–137.
[25] S. Lindskog, Pharmacology and Therapeutics 74 (1997) 1–20.
[26] S.Z. Fisher, C.K. Tu, D. Bhatt, L. Govindasamy, M. Agbandje-McKenna, R. McKenna, D.N. Silverman, Biochemistry 42 (2007) 3803–3813.
[27] G.S. Jacob, R.D. Brown, S.H. Koenig, Biochemical and Biophysical Research Communications 82 (1978) 203–209.
[28] I. Simonsson, S. Lindskog, European Journal of Biochemistry 123 (1982) 29–36.
[29] Y. Pocker, C.H. Miao, Biochemistry 26 (1987) 8481–8486.
[30] K. Hakansson, A. Wehnert, Journal of Molecular Biology 228 (1992) 1212–1218.
[31] D.W. Christianson, C.A. Fierke, Accounts of Chemical Research 29 (1996) 331–339.
[32] S. Lindskog, in: T.G. Spiro (Ed.), Carbonic Anhydrase, John Wiley & sons, New York, 1983, pp. 78–121.
[33] G. Navon, H. Shinar, Inorganica Chimica Acta-Bioinorganic Chemistry 46 (1980) 51–55.
[34] K.B. Schowen, R.L. Schowen, Methods in Enzymology 87 (1982) 551–606.
[35] Z. Fisher, J.A. Hernandez Prada, C. Tu, D. Duda, C. Yoshioka, H. An, L. Govindasamy, D.N. Silverman, R. McKenna, Biochemistry 44 (2005) 1097–1105.